Fish & Shellfish Immunology 62 (2017) 13–23

Contents lists available at ScienceDirect

Fish & Shellfish Immunology

journal homepage: www.elsevier.com/locate/fsi

Full length article

Transcriptome profiling of spleen provides insights into the antiviral mechanism in *Schizothorax prenanti* after poly (I: C) challenge

Xiaogang Du [a, *, 1], Yunkun Li [a, 1], Dong Li [a], Fangliang Lian [a], Shiyong Yang [b], Jiayun Wu [c], Hanmei Liu [a], Guixian Bu [a], Fengyan Meng [a], Xiaohan Cao [a], Xianyin Zeng [a], Huaiyu Zhang [a], Zhiyu Chen [a]

[a] Department of Engineering and Applied Biology, College of Life Science, Sichuan Agricultural University, Ya'an 625014, Sichuan, China
[b] Department of Aquaculture, Sichuan Agricultural University, 625014, Sichuan, China
[c] Department of Zoology, Sichuan Agricultural University, 625014, Sichuan, China

ARTICLE INFO

Article history:
Received 17 November 2016
Received in revised form
27 December 2016
Accepted 4 January 2017
Available online 4 January 2017

Keywords:
Transcriptome
Schizothorax prenanti
poly (I:C)
Differential expressed genes
Spleen
qPCR

ABSTRACT

Schizothorax prenanti (*S. prenanti*) is an important economical cold-water fish species in southwestern China, but it is susceptible to various pathogens infection. In order to clearly elucidate the antiviral mechanism, in this study, we have analyzed the transcriptome of *S. prenanti* spleen after challenge with the virus mimic, poly (I:C) (pIC), using next generation sequencing technology (RNA-seq). A total of 313 differential expressed genes (DEGs) in spleen at 12 h were obtained after pIC treatment, including 268 significantly up-regulated unigenes (fold change > 2) and 45 significantly down-regulated unigenes (fold change > 2). Through the immune-related DEGs (IRDs) screening, 47 IRDs were used to establish heat map, which intuitively showed a significantly difference after pIC treatment. To validate the RNA-seq data and observe gene expression, the expression levels of 14 IRDs were detected by qPCR after pIC treatment at 0, 4, 8, 12, and 24 h. The results indicated that the qPCR data presented a positive line correlation with RNA-seq data, and the 14 IRDs were responsive to pIC stimulation except IL-1β. Thus, based on the RNA-seq and qPCR data, we inferred that MDA5- and Jak-mediated signaling pathways may involve in the antiviral signaling transduction, and induce type I IFNs and ISGs to block virus invasion, respectively. Unfortunately, TLR3 and TLR22, as receptors of virus dsRNA, were no significantly expressed in this study. Nonetheless, our study still provides useful mRNA sequences of antiviral immunity for further immunological research, and facilitates improving disease restriction in *S. prenanti*.

1. Introduction

Recently, *S. prenanti* has attracted a lot of attention due to its taste, nutrients and high commercial value. It is widely distributed in the upper reaches of Yangtze river. With the development of industrial farming, *S. prenanti* becomes an important cold-water fish, which creates enormous economic value. However, intensive feeding always easily leads to outbreaks various diseases induced by viruses and bacteria such as *aeromonas hydrophila* [1], *streptococcus agalactiae* [2], reovirus and hematopoietic necrosis virus [3], which causes economic losses. In order to establish the reasonable measures that can control diseases and reduce the risk of aquaculture, clearly identifying diseases defensing mechanism is extremely required. Previous studies on *S. prenanti* mainly focused on immunomodulator and cloning of immuno- and reproduction-related genes [4–7]. Meanwhile, because of absence of understanding of the genetic background of *S. prenanti*, little valuable data have been provided to understand pathogens defensing mechanism, especially for antiviral immunity. Hence, we have investigated genes expression of the organism defensing against virus infection, which relies on it that pathogen-associated molecular patterns (PAMPs) are recognized by pattern recognition receptors (PRRs), and that performs by the innate immune system [8].

Innate immune system plays a crucial role in the organism defense response to confine virus/bacteria invasion [9]. Innate immunity is characterized by PRRs to bind specific pathogen molecules, also known as PAMPs, including various types of bioactive glycans and microbial nucleic acids [10]. RIG-I-like

* Corresponding author.
E-mail address: duxiaogang@sicau.edu.cn (X. Du).
[1] the authors contributed to this work equally.

http://dx.doi.org/10.1016/j.fsi.2017.01.004
1050-4648/

receptors (RLRs), Toll-like receptors (TLRs), NOD-like receptors (NLRs), and C-type lectin receptors (CLRs) are the four major receptor systems for PRRs to combine kinds of PAMPs. In antiviral response, virus elements including double-stranded RNA (dsRNA), single-stranded RNA (ssRNA) and DNA are primary recognized by TLRs and RLRs, and activate the type I interferons(IFNs) response by a series of downstream signaling cascades [11,12].

To date, it has been well accepted that TLRs are comprised of 20 subfamilies in fish, but only 10 subfamilies in mammals [13,14]. Among 20 TLRs in fish, TLR3, 7, 8, and 9 exclusively recognize virus specific ligands in intracellular endosome: TLR3 recognizes dsRNA, while TLR7 and TLR8 recognize ssRNA, and TLR9 recognizes unmethylated CpG DNA of virus [9,15–17]. RLRs are also called RLHs because their DExD/H RNA helicases domain can senses viral dsRNA/DNA in cytoplasm [18–20]. The retinoic acid-inducible gen I (RIG-I), melanoma differentiation-associated protein 5 (MDA5), and laboratory of genetics and physiology 2 (LGP2) are the three major members of RLRs family, which induce the initialing signaling to activate downstream signaling cascades [21]. RIG-I and MDA5 recognize short dsRNA (less than 300 bp) with 5'-triphosphorylated ends (5′-PPP) and long dsRNA (more than 1000 bp) without ends specific fraction, respectively [20,22,23]. In contrast, since lacking of CARDs domain, LGP2 can not directly interact with virus components, and plays broad regulation in RLRs-mediated antiviral responses [24–27]. Furthermore, RIG-I and MDA5 align with IFN-β promoter stimulator 1 (IPS-1), which associates with TNF-receptor-associated factor 3 (TRAF3). Thereby, TRAF3 recruits TANK-binding kinase 1 (TBK 1) and IκB kinase (IKKε), following activating interferon regulation factor 3/7 (IRF 3/7), which results in the induction of type I IFN genes and subsequent IFN stimulated genes (ISGs) to block viral invasion [21,28–30].

In this study, we used the pIC, a kind of double-stranded RNA, to imitate viral invasion. Subsequently, we identified for the first time DEGs between pIC and control group based on RNA-seq. Meanwhile, GO and KEGG enrichment analysis of DEGs that exposed the biological effects of pIC were picked out. Finally, we screened out the IRDs, verified the RNA-seq data by qPCR, and predicted the signaling transduction of the antiviral immunity.

2. Materials and methods

2.1. Fish and pIC

S. prenanti with an average weight of about 350 g, was purchased from Ya-fish Company (Ya'an, china). Each fish was acclimatized for two weeks in 70 cm × 50 cm × 46 cm fiberglass tanks with no chlorine freshwater at 20 °C, natural photoperiod (12L:12D). pIC was obtained from Sigma-Aldrich Co. (St. Louis, MO, USA), and stored in −20 °C until challenge experiment. All procedures of handling the animals were performed in accordance with the protocols approved by the Animal Protection Committee of Sichuan Agricultural University.

2.2. Total RNA extraction, library construction and sequencing

Twenty healthy *S. prenanti* were randomly divided into two groups including PBS and pIC challenge group. Each fish was sacrificed at 12 h after intramuscular injection of 5 mg per 1 kg body weight pIC or isochoric PBS. Total RNA was extracted from spleens by EASYspin Plus kits (Aidlab Biotech, Beijing, China), and all operations strictly followed the manufacturer's instruction. Concentration and purity of total RNA were measured by NanoDrop spectrophotometer (Thermo, USA) and gel electrophoresis, respectively. 10 RNA samples of each group were pooled together for RNA sequencing.

In the stage of sequencing, mRNA was randomly digested into small pieces by fragmentation buffer, and enriched by magnetic beads with Oligo (dt). Subsequently, the first-strand cDNA was synthesized using the mRNA pieces as templates, and the complementary strand was synthesized. Then, the intact cDNA was purified, processed with AMPure XP beads, and connected with "A" tail and adaptors for PCR amplification. The library was acquired after cDNA was purified by the AMPure XP beads. Finally, the insert size of library was sequenced by using an Illumina Hiseq 2500 platform and sequencing progress was accomplished by Novogene (Beijing Novogene Technologies, Beijing, China).

2.3. Transcripts assembly and annotation

In order to prepare clean reads for transcripts assembly, raw reads were filtered by discarding previous adapters and low quality reads. The *de novo* assembly of RNA-seq was performed by using Trinity software, which was developed by Broad Institute and Hebrew University of Jerusalem, and contains three independent components: Inchworm, Chrysalis and Butterfly [31]. Inchworm was used to disassemble reads, constructed K-mer (K = 25) dictionary, and selected K-mer for bidirectional extension, resulting in the formation of contigs. Chrysalis aggregated overlapped contigs for constituting components, which have several de Bruijn graph. Each de Bruijn graph of the components was simplified by Butterfly, also exported full-length transcripts of alternative splicing type and teased the corresponding transcripts of paralogs. At last, the longest transcript of each gene was regarded as unigenes.

Unigenes were used for Blast and annotation against seven databases, including Nr, Nt, Pfam (http://pfam.sanger.ac.uk/), KOG/COG (http://www.ncbi.nlm.nih.gov/COG/), Swiss-prot (http://www.ebi.ac.uk/uniprot/), KEGG (http://www.genome.jp/kegg/) [32], GO (http://www.geneontology.org/) [33], using an E-value cut-off of 10^{-5}.

2.4. Screening IRDs

After annotations, unigenes expression levels were calculated by a RSEM software [34], and the FPKM-values represent expression levels [35]. DEGs of pIC and PBS group were decided within q-Value< 0.005, $|\log_2(\text{fold change})| > 1$. Meanwhile, the clusters of GO and KEGG analysis were marshalled, according to Cluster frequency within Corrected-p-Value < 0.05. Subsequently, the IRDs were screened basing on that who involved in immune-associated pathways such as Jak-stat, RIG-I/MDA5 and TLR signaling pathway and so on. Heat map of the selected DEGs was mapped by HemI software (http://hemi.biocuckoo.org/) [36].

2.5. Validating the RNA-seq data and observing gene expression by qPCR

After injection with PBS or pIC (n = 10) at 0, 4, 8, 12 and 24 h, 100 *S. prenanti* from 10 groups were sacrificed for qPCR analysis. The quality of mRNA sample was determined by absorbance of 260/280 nm and agarose gel electrophoresis. Reverse transcription reactions were performed by the PrimeScripy® RT reagent kit with gDNA Eraser (Takara Bio, Co. Ltd., Dalian, China). Then, the qPCR was performed by using SYBR® green II (Takara Bio Co. Ltd., Dalian, China) with the cDNA as template, following conditions: 95 °C for 3 min; 40 cycles of 95 °C for 5 s and several annealing temperature for 30 s; 95 °C for 10 s; melt curve detection of 65 °C for 5 s to 95 °C increment 0.5 °C. The forward and reverse primers were shown in Table 1. RNA expression levels were calculated as fold changes by normalizing to β-actin reference gene.

Table 1
Primes used for qPCR validation of immune-related DEGs.

Unigenes name	Primes sequence 5′ to 3′		Ta opt (°C)	Length (bp)
CXL11-1	Forward	CTGTGTTTAAGCATCTTCGACCG	51.8	118
	Reverse	ATGGTGAAGCCAAAGCTGATAGAG		
CXL11-2	Forward	GATGGACTTGGAGGGATGATTTC	53.3	142
	Reverse	TTCTTCTCGCCTGCCTGATG		
IL-1β	Forward	ATTTGAAGGCTGTGACGCTGAG	53.9	180
	Reverse	TCAAGAGCAGGACGGGAGAAG		
IL-10	Forward	TTCGTTCAGTAATGGTTCCAAGTCA	51.8	103
	Reverse	TGTGGAGGGCTTTCCTGTGAG		
IRF1	Forward	TCATGGCACAGCGGAAATTG	53.7	122
	Reverse	CTGGGAGGTGGATAAAGACGC		
IRF7	Forward	TGAGGACGGATGATGCGATAG	51.7	127
	Reverse	ACGACAAAGCGAAATGGAAGAC		
IRF8	Forward	CACGCTTTGAAGATGGACGC	53.3	104
	Reverse	CTGCTATGGGAGGATGAGAACC		
IRF9	Forward	CACAGTTGGACATCTCAGAACCCTA	54.3	132
	Reverse	CACAGTTGGACATCTCAGAACCCTA		
LGP2	Forward	ATTTCACGCCCACCTTCTTCA	56.0	177
	Reverse	CCTCAACCTCCTCATCTCCACC		
LTA	Forward	ACGGATGCGGTGGAAGAGTG	55.4	115
	Reverse	GCTTAAAGACAGCGCCCAGGTA		
MDA5	Forward	TGCAGGAGTTGATGGGAAAGC	53.6	121
	Reverse	CGGGTCCGGGTGAATATGAT		
PKR	Forward	GCAGTCACGAGACCGAAGT	56.0	175
	Reverse	CAGATGTTGATTACCCAGAG		
PKZ	Forward	CCTTGGGCTCGTATGGTTTG	52.9	172
	Reverse	TGGCCTGTGCTCTGGTGAA		
STAT1	Forward	TATTTCCTTGCCAAACGTCATCC	54.4	119
	Reverse	AGTAGCGACCGAAGGCGACA		
TRAF3	Forward	ATCTACTCAAACCTCCTCCA	55.0	102
	Reverse	TGAGCCGTCAGCTTGTGC		
β-actin	Forward	TGTTCCAGCCTTCCTTCATTG	52.5	120
	Reverse	CAGACAGGACGTTGTTGGCATA		

3. Results

3.1. De novo assembly and function annotation

About 54 million clean reads in PBS sample and 55 million clean reads in pIC sample were obtained after filtering out redundant and short reads [Table 2]. The quality of clean reads showed that the error was less than 0.01%, the Q30 was high than 93%, and the content of G/C was approximately equal (47%) per library. All clean reads were spliced into 221, 963 transcripts with mean length of 827 and N50 length of 1, 716. 16, 3651 unigenes with mean length of 630 and N50 length of 1, 045 were validated [Table 3]. These results indicate that the sequencing data are high-quality, and the unigenes can be used for subsequent annotation analysis.

In order to learn genes function information comprehensively, 100, 063 unigenes were annotated by seven databases including Nr, Nt, KOG/COG, Swiss-prot, KEGG and GO. The success rate of annotation showed that 40, 347 of unigenes were matched in Nr, 139, 448 in Nt [Table 4]. In Nr annotation, 40, 347 unigenes were matched to multiple species genomes, including *Danio rerio* (64.1%), *Astyanax mexicanus* (4.6%), *Oncorhynchus* (2.6%), *Larimichthys crocea* (2.1%), *Clupea harengus* (1.8%), and other (24.7%). Meanwhile, protein sequences with high similarity to known genes in Swiss-prot were 31, 158. In total, 143, 545 unigenes were successful matched in at least one database, while 10, 386 unigenes were matched in all databases.

Table 2
The quality of clean reads.

Sample	Clean reads	Error(%)	Q20(%)	Q30(%)	GC content(%)
pIC	55,162,876	0.01	97.29	93.28	46.91
PBS	53,892,940	0.01	97.46	93.61	47.06

3.2. Identification of DEGs after pIC treatment

All of unigenes were analyzed by DEG-seq whose threshold was restricted in q-value < 0.005, $|\log_2(\text{foldchange})| > 1$. 313 unigenes were identified as DEGs containing 268 significantly up-regulated and 45 significantly down-regulated unigenes. DEGs were visually observed in volcano plot at 12 h after pIC treatment (Fig. 1). In the volcano plot, we also observed that the up regulation levels of DEGs were significantly higher than the down regulation levels.

3.3. GO and KEGG enrichment analysis of DEGs

To further investigate the function of DEGs, all DEGs were classified into three gene ontology categories (Biological process,

Table 3
The distribution of splicing length.

	Number	Mean length	Median length	Max length	N50	N90
Transcripts	221,963	827	369	27,100	1716	285
Unigenes	163,651	630	318	27,100	1045	248

Table 4
The statistics of success rate of annotation.

	Number of unigenes	Percentage (%)
Annotated in NR	40,347	24.65
Annotated in NT	139,488	85.23
Annotated in KOG	18,691	11.42
Annotated in SwissProt	31,158	19.03
Annotated in PFAM	32,689	19.97
Annotated in GO	33,750	20.62
Annotated in KEGG	18,146	11.08
Annotated in all Databases	10,386	6.34
Annotated in at least one Database	143,545	87.71
Total Unigenes	163,651	100

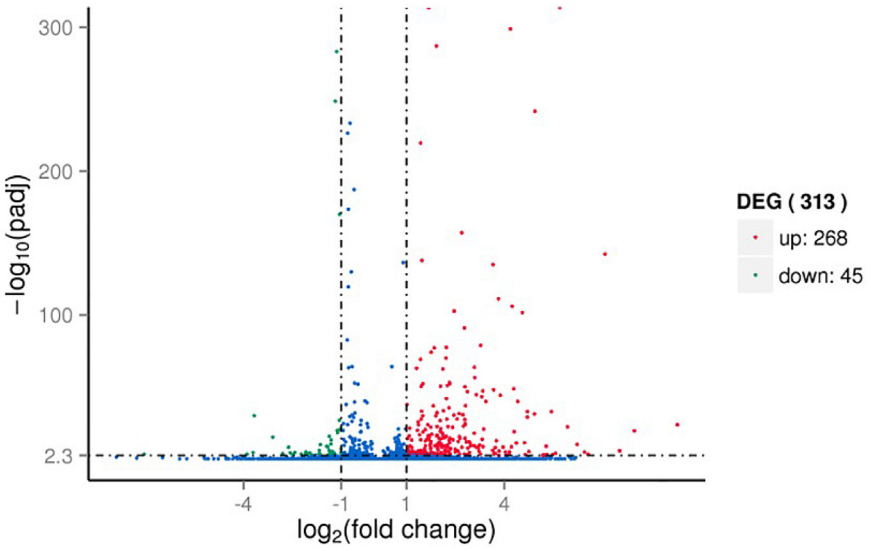

Fig. 1. Volcano plot of differential expressed genes comparing of pIC and PBS group. The X-axis represents fold change between pIC and PBS group, the Y-axis indicates significance of differential expression. The blue pots mean no significantly change unigenes ($P < 0.05$, false discovery rate (FDR) $q < 0.05$), while the red pots and the green pots mean up- and down-regulated unigenes ($P < 0.05$, FDR $q < 0.05$), respectively. (For interpretation of the references to colour in this figure legend, the reader is referred to the web version of this article.)

molecular function and cellular component) by the Blast2GO. Interestingly, in this study, DEGs were only assigned to biological process (BP) and molecular function (MF) ($P < 0.05$, FDR<0.01), comprised of 19 and 7 subcategories, respectively (Fig. 2). Among the biological process, the top three clusters frequency were "biological regulation" (43.1%), "regulation of biological process" (42%), and "regulation of cellular process" (40.1%). Moreover, some terms of biological process were closely related to immune response such as "immune response" ($P < 0.001$, 6.3% of cluster frequency) and "immune system process" ($P < 0.001$, 7.4% of cluster frequency). In the molecular function classes, "cytokine receptor binding" (5.2%), "chemokine activity" (3.0%) and "chemokine receptor binding" (3.0%), were constituted the top three cluster frequency with all of the *P*-value less than 0.001, indicating emergence of a complex antiviral immune response after pIC treatment.

Within the KEGG annotation, the top 20 pathways were shown in Fig. 3. Significantly, DEGs were assigned to the comprehensive host defense signaling pathways, which were related to various

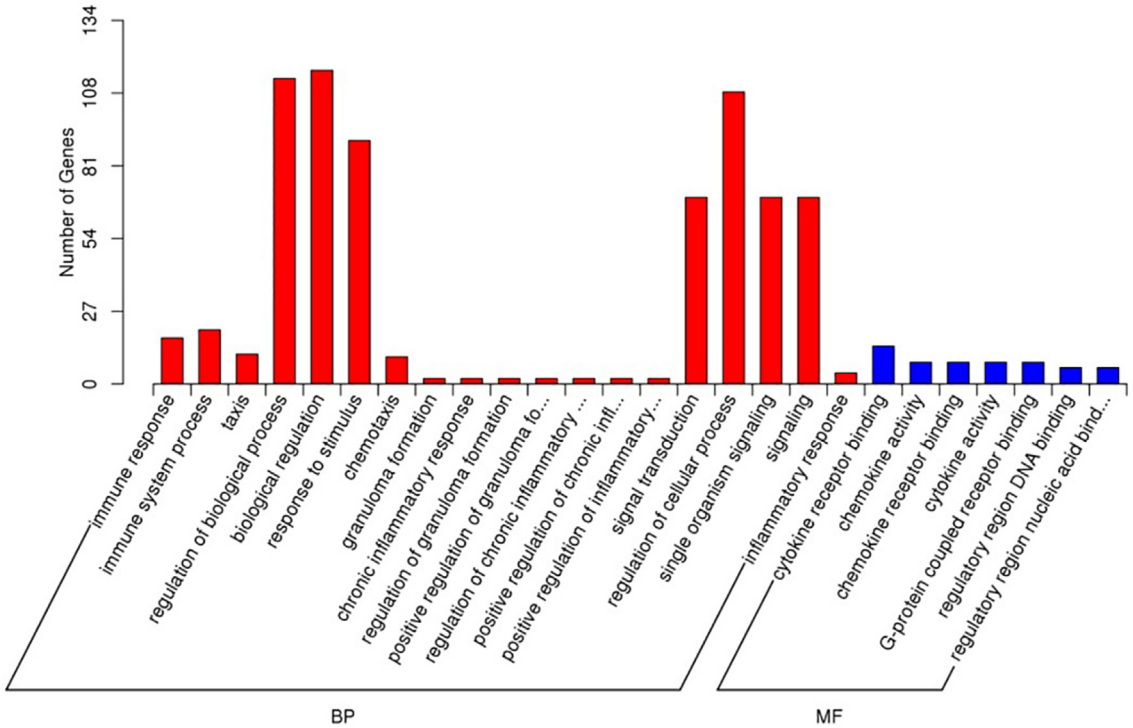

Fig. 2. Histogram description of Gene Ontology enrichment of DEGs. All the DEGs were fell into two categories: biological process (BP) and molecular function (MF). The X-axis represents various gene function, the Y-axis corresponds to the number of DEGs.

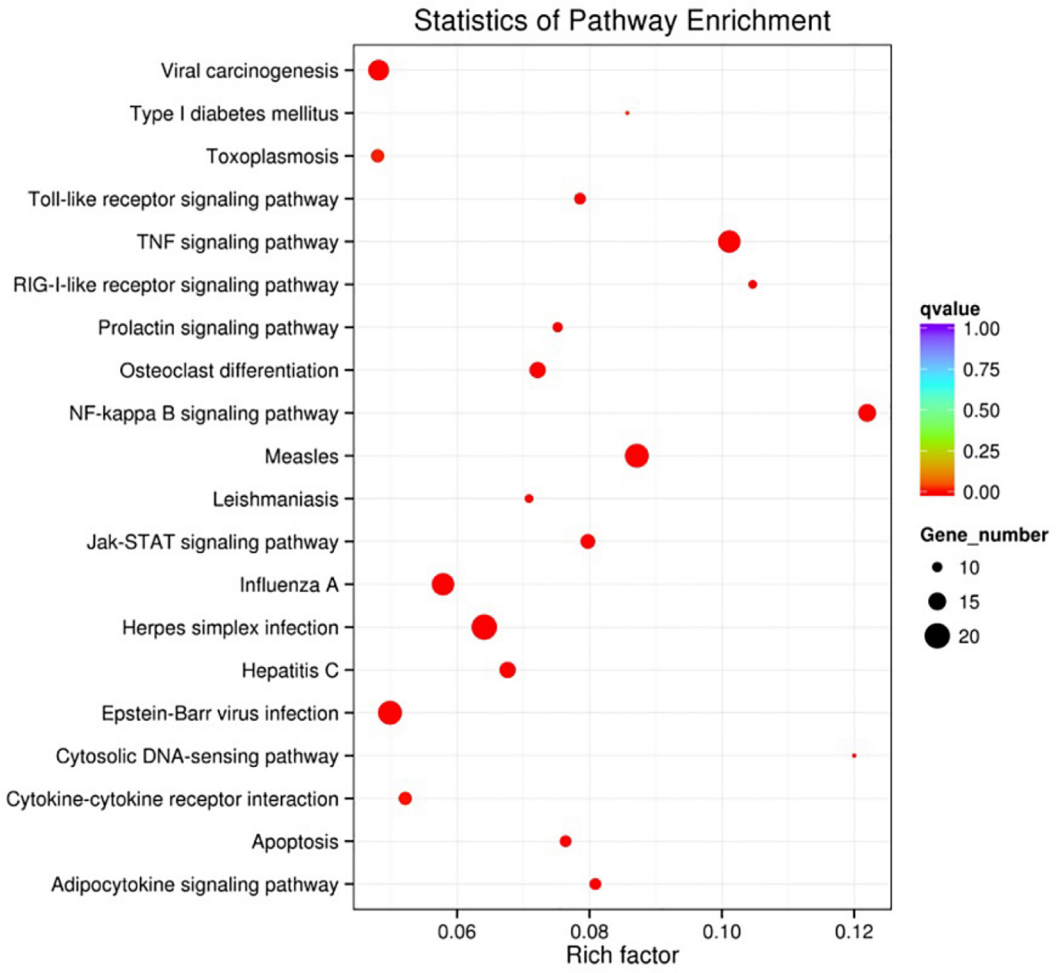

Fig. 3. Scatter diagram of pathway enrichment for DEGs. In this scatter diagram, the top 20 pathways were listed, and rich factor is the ratio of DEGs in this pathway to all the genes in this pathway. The X-axis corresponds to rich factor of pathway, and the Y-axis represents different pathway. The magnitude of the pots displays gene number ranged from 10 to 20, and q-value is described by the color classification. (For interpretation of the references to colour in this figure legend, the reader is referred to the web version of this article.)

antiviral responses, such as “herpes simplex infection”, “epstein-barr virus infection”, “RIG-I-like receptor signaling”, “toll-like receptor signaling pathway” and so on. Among these antiviral pathways, we focused on the dominant antiviral-related signaling pathways such as RLR- and TLR-mediated signaling pathways, which were regarded as reference to screen IRDs.

3.4. Heat map of IRDs

After identification and annotation of DEGs, most of DEGs were compactly relate to immune response. In order to explore the antiviral mechanism comprehensively, a series of DEGs were identified as IRDs which involved in antiviral signaling cascades such as TLR- and RLR-mediated signaling pathways, as well as various diseases pathways. Subsequently, 47 IRDs were screened, and distributed in heat map (Fig. 4). Among 47 IRDs, most of IRDs were varying degrees of up-regulated after pIC treatment. Approximate 34% of IRDs involved in TLR- and RLR-mediated signaling pathways, which play a crucial role in type I IFNs response activated by specific ligands of virus/bacteria. Five members of interferon regulation factors (IRFs) family (IRF1, 2, 7, 8, and 9) were screened, which may provide insights into antiviral immunity mediated by the recognition of PAMPs in surface/cytosolic [37,38]. In addition, a series of chemokines, cytokines, complements, and other signaling transduction molecules also had high expression levels in this study. Finally, we selected 14 IRDs, which may uncover the antiviral mechanism, to validate the RNA-seq data by using qPCR.

3.5. Validation of the RNA-seq data and detection of the mRNA expression by qPCR

The expression levels of 14 IRDs were detected by qPCR at different time points (0, 4, 8, 12 and 24 h), as shown in Fig. 5 and 6, 13 IRDs were responsive to stimulation of pIC at 4, 8, 12 and 24 h, but IL-1β was no significantly up-regulated at each time point. Two unigenes were matched to C-X-C motif chemokine 11 (CXCL11) by Nr Blast, named CXCL11-1 and CXCL11-2, which were significantly up-regulated after pIC-injected at 4 and 8 h (Fig. 5a and b). The IL-10 was significantly up-regulated at each time point, while the IL-1β was markedly down-regulated at 4 h and not impacted at residual time points. Subsequently, we further detected the expression levels of 10 well-known effectors which involved in the antiviral signaling transduction (Fig. 6). The results showed that these crucial components of organism defensing transduction cascades are responsive to stimulation of pIC, especially for IRF7, LGP2, PKZ and STAT1, which presented higher expression levels in this study.

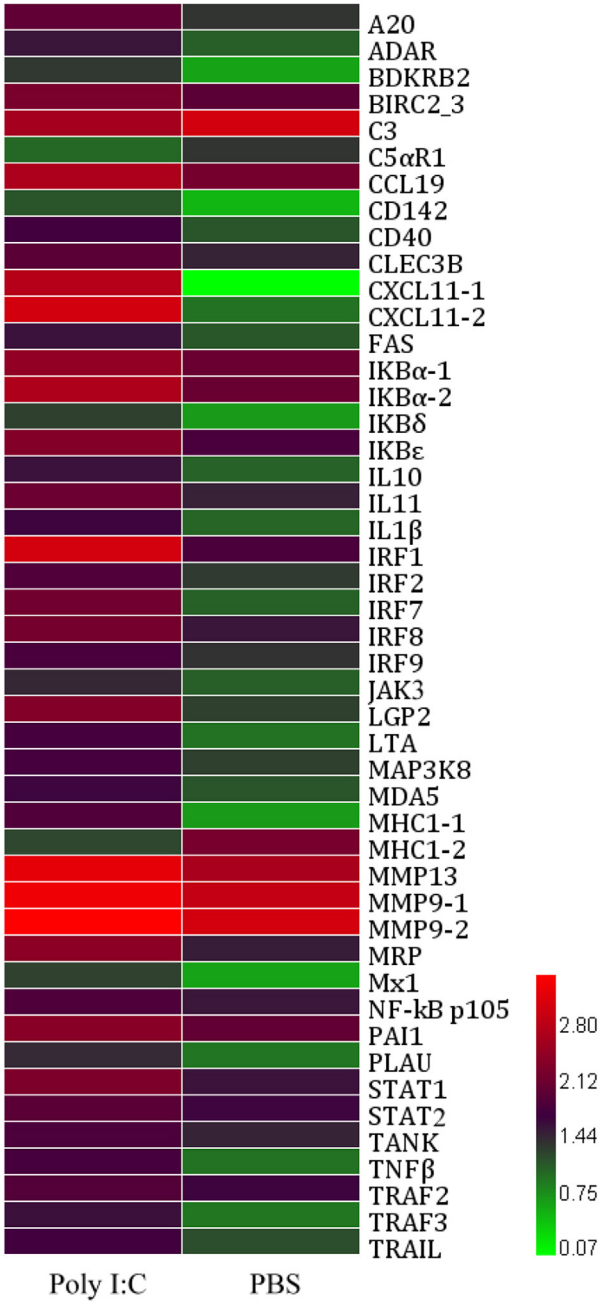

Fig. 4. Heat map of IRDs. The expression levels of IRDs closely relate to host defensing signaling pathway after pIC treatment in *S. prenanti* spleen. The heat map was performed based on FPKM of RNA-seq data, and represents the unigenes expression levels. The expression levels of IRDs are divided into various classification in the bar according to $\log_{10}$(FPKM) value. The red region indicates high expression levels in challenge to legend stimulation. The green region indicates low expression levels in challenge to legend stimulation. (For interpretation of the references to colour in this figure legend, the reader is referred to the web version of this article.)

To validate the reliability of the RNA-seq data, we have analyzed the correlation between RNA-seq data and qPCR data at 12 h (Fig. 7). The results showed the qPCR data presented a positive line correlation with RNA-seq data, indicating that the data of RNA-seq data are desirable.

3.6. Prediction of the antiviral signaling transduction

Based on RNA-seq data and knowledge of antiviral signaling pathways in teleost, a putative draft of the antiviral signaling pathway focused on MDA5- and Jak-mediated pathways was constructed (Fig. 8). In this map, we deduced that the antiviral immune response in *S. prenanti* may activate MDA5- and JAK-mediated signaling pathways, and induce type I IFNs and ISGs to block virus invasion, respectively. Unfortunately, TLR3 and TLR22, as receptors of virus dsRNA, were not significantly expressed in this study. In addition, whether IRF1 and IRF8 directly involved in the signaling initiation/transduction remains to be investigated in future study.

4. Discussion

S. prenanti is a famous cold-water fish with enormous economic value in southwestern China. The extensive feeding of *S. prenanti* easily leads to outbreaks various diseases, which causes economic losses. Therefore, it is necessary to illuminate the molecular mechanism of disease defensing in *S. prenanti* for decreasing economic losses of fisherfolk. In this study, we have picked up the transcriptome comparative data of *S. prenanti* spleen after pIC treatment. 100, 063 unigenes were acquired after assembling and filtration. Each unigene was annotated based on seven databases, and the results showed that only 31, 158 (19.3%) and 40, 347 (24.65%) unigenes were matched in SwissProt and Nr databases, respectively. However, approximately 20,106 (12.29%) unigenes failed to identify via these protein databases. As for the unidentified unigenes, we presumed that there are two reasons: some unigenes' information is still unknown and the blast tools are limited at special parameter containing small gaps and low error rate.

In present study, we identified 313 DEGs using DEG-seq analysis by comparison of pIC- and PBS-injected in *S. prenanti* spleen. Among 313 DEGs, 268 DEGs were significantly up-regulated, while the remaining DEGs were significantly down-regulated. Besides, Go enrichment analysis of the DEGs revealed that most of the DEGs were enriched in biological process such as “biological regulation” (43.1%), “regulation of biological process” (42%), and “regulation of cellular process” (40.1%). This functional distribution suggests that pIC can activate the organism defensing response in *S. prenanti*, and these DEGs may play an important role in the signaling transduction of elimination of external stimulus. After KEGG analysis of DEGs, the top 20 pathways were described in Fig. 3, suggesting a strong antiviral immune response is activated in *S. prenanti*. DEGs enriched pathway showed that various antiviral signaling pathways were activated after pIC treatment, such as TLR- and RLR-mediated signaling pathways, which are the two major signaling pathways implicated antiviral response to block virus invasion [12]. Meanwhile, some DEGs were assigned to complicated antiviral pathways containing “influenza A” and “Herpes simplex infection”, which are similar to pIC-stimulated in miiuy croaker [39]. Therefore, we inferred that *S. prenanti* are susceptible to virus in artificial feeding, and perform a comprehensive antiviral immune response against virus infection.

Currently, we have screened 47 IRDs, which directly involve in the immune-related pathways according to the results of KEGG analysis. The heat map of 47 IRDs in Fig. 4 highlighted a large fold change after pIC treatment. Many IRDs are well-known immune effectors, including RLR and IRF family members, which can induce the type I IFNs (IFNα/β). Previous studies have demonstrated that the RLR members like MDA5 recognize dsRNA with the assist of LGP2, and IRF family in fish presents a positive regulation in antiviral immunity [22,23]. For instance, IRF7 was reported as a key regulator in MDA5-mediated pathway to induce the expression of type I IFNs (IFNα/β) [40–42]. In addition, some signaling molecules of Jak-stat signaling pathway, such as IRF9, STAT1 and STAT2, were significantly up-regulated. According to previous studies, these molecules indirectly/directly mediate the production of ISGs by

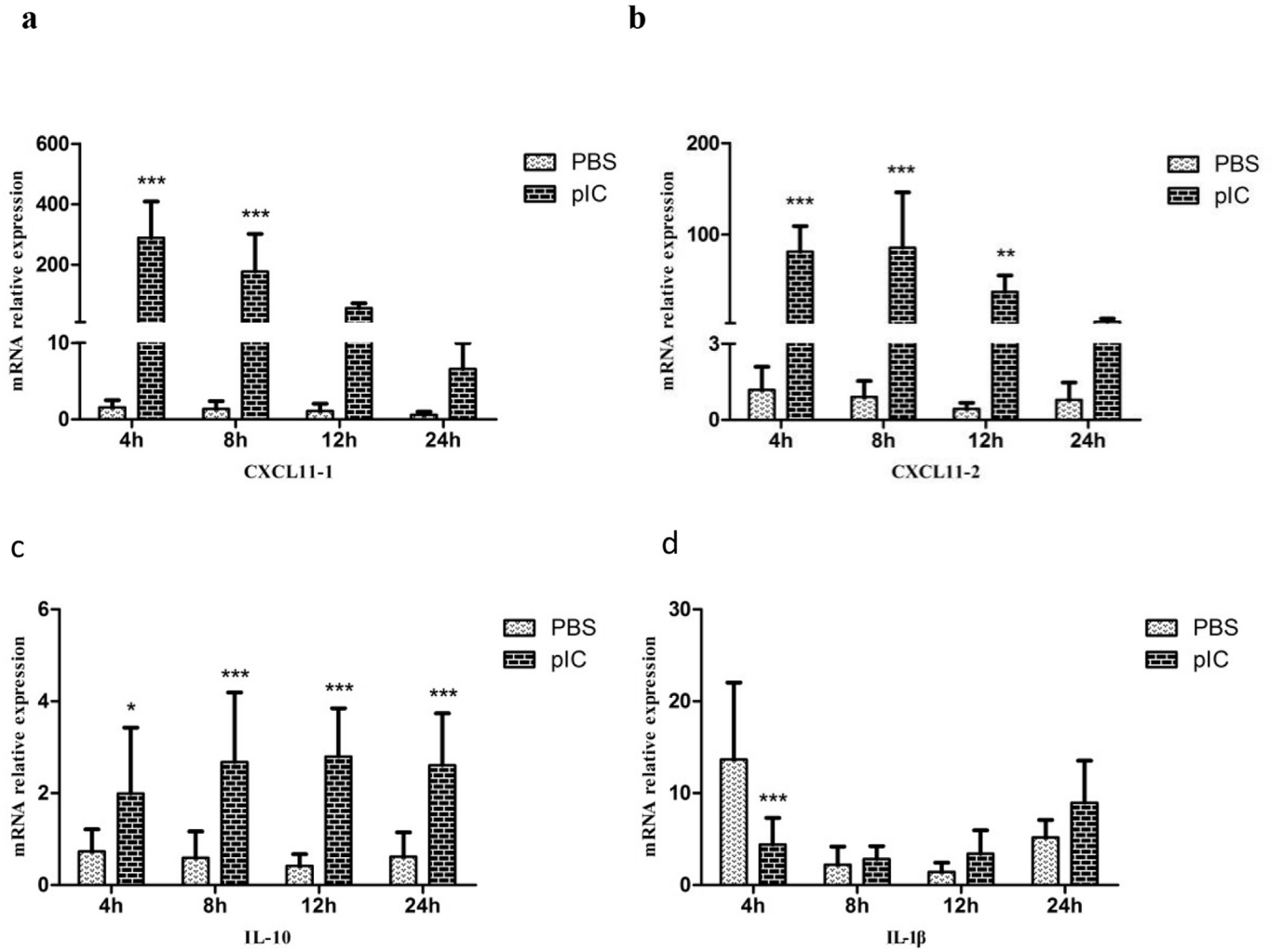

Fig. 5. qPCR results of cytokine and chemokine in spleen after pIC treatment. (a) CXCL11-1; (b) CXCL11-2; (c) IL-10; (d) IL-1β. Data are shown as the mean average ± SD (n = 10). $^{*}P < 0.05$, $^{**}P < 0.01$, $^{***}P < 0.001$ vs. corresponding time point of PBS group; two-way ANOVA plus Bonferroni post- tests.

type I IFNs, thereby to restrict the replication of virus [43,44]. Therefore, based on these data, we selected several IRDs, which indirectly/directly involve in MDA5- and Jak-mediated signaling pathways, for subsequent qPCR validation.

In teleost, the innate immune system heavy relies on the initial response against pathogen, and the adaptive immune system is restricted in suboptimal environments [45]. Type I IFNs response plays an important role in the innate immunity, and the repertoires of signaling transduction of it is induced by TLRs and RLRs [46,47]. In this study, we mainly focused on the IRDs, which involve in type I IFNs response signaling cascades, and the expression levels of 14 IRDs were detected via qPCR at 4, 8, 12, 24 h after pIC treatment. Chemokines are generally believed to be a subfamily of chemotactic cytokines, and have broad spectrum of effects on the innate immunity, such as becoming a promoter to adhere various types of leukocyte to inflammatory loci in early immunity [48,49]. In *S. prenanti*, CXCL11-1 and CXCL11-2 were significantly induced at 4 and 8 h after pIC treatment, suggesting that pIC can induce a robust early immune response. In mammals, IL-10 plays a central role in anti-inflammatory response, and traditionally acts as an inhibitor of immune response such as decreasing the production of pro-inflammatory cytokines from $CD4^{+}$ T cells [50–52]. Consistently, in teleost, it was reported that the recombinant goldfish IL-10 reduced the expression of pro-inflammatory factor, including TNFα1, TNFα2, and IL-1β in monocytes [53]. To our knowledge, these inflammatory factors sever as protective properties to remove the adverse stimulus in the first line of organism defensing against virus invasion, but more strong inflammatory response can lead to tissue damage as well. In our study, IL-10 was markedly up-regulated, which revealed that IL-10 may decrease inflammatory damage induced by virus via keeping the balance of immune system. This may be the reason why no significantly up regulation of IL-1β was detected at each time point. Moreover, the result of IL-1β is similar to what reported in Atlantic cod macrophages after pIC treatment [54].

We also found that 4 IRFs (IRF1, 7, 8, 9) were responsive to pIC stimulation compared to PBS stimulation. IRF1 and IRF7 have a uniform function in the regulation of type I IFNs production by directly binding to IFNα/β promoters [55,56]. In addition, IRF7 is described as a main regulator to induce the expression of IFNα/β in MDA5-mediated signaling cascades [42]. Both of IRF1 and IRF7 were significantly up-regulated at each time point, suggesting that type I IFNs response is induced in this study. Interestingly, IRF1 was induced in the early phase of antiviral response, while IRF7 was induced with time dependency. What's more, IRF7 presented a large fold change at each time point compared to IRF1. These results indicate IRF1 and IRF7 may act as different role in the activation of type I IFNs, but the mechanism will need to be study in future.

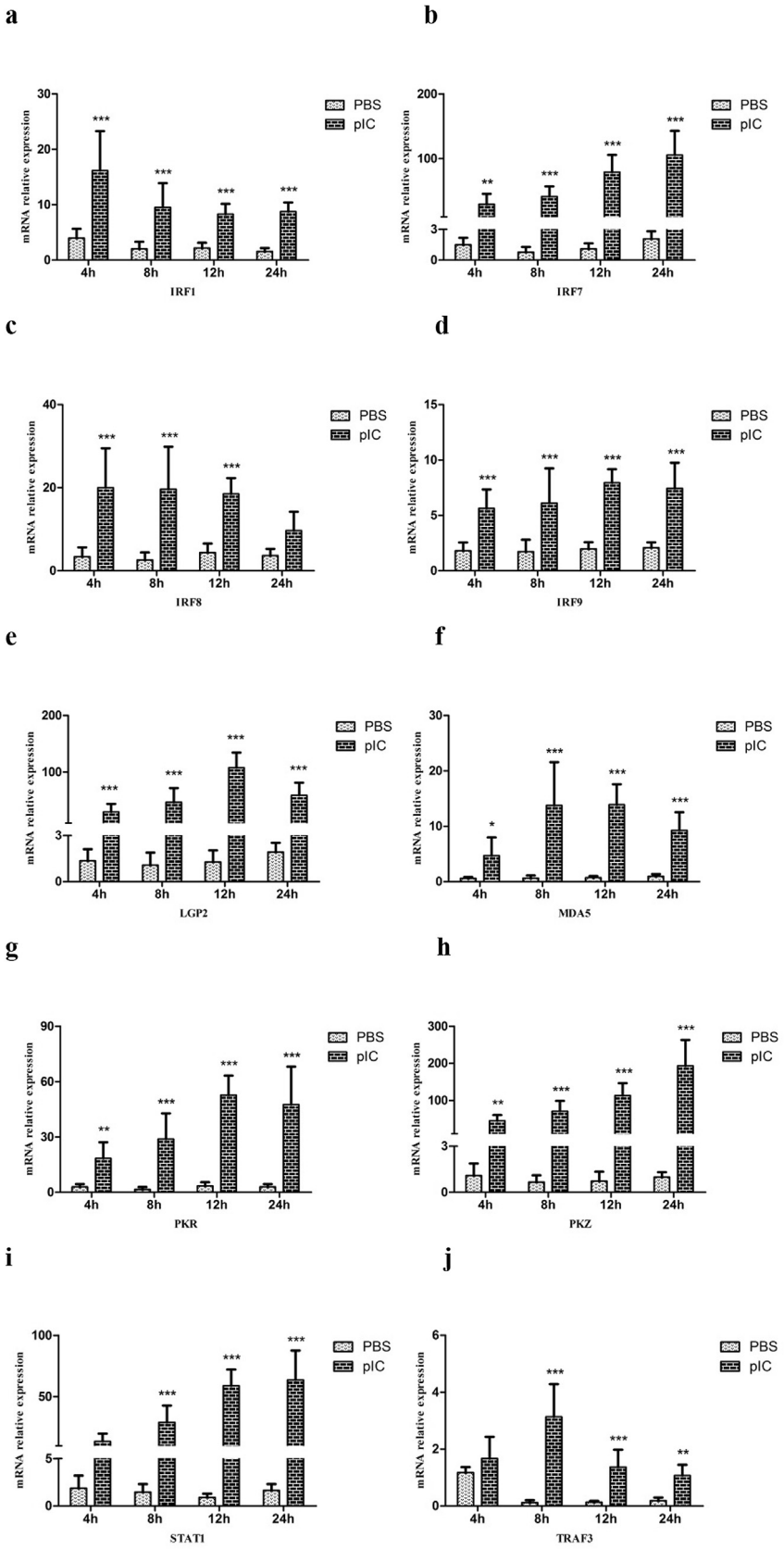

Fig. 6. qPCR results of well-known immune effectors in spleen after pIC treatment. (a) IRF1, (b) IRF7, (c) IRF8, (d) IRF9, (e) LGP2, (f) MDA5, (g) PKR, (h) PKZ, (i) STAT1, and (j) TRAF3. Data are shown as the mean average ± SD (n = 10). $^{*}P < 0.05$, $^{**}P < 0.01$, $^{***}P < 0.001$ vs. corresponding time point of PBS group; two-way ANOVA plus Bonferroni post- tests.

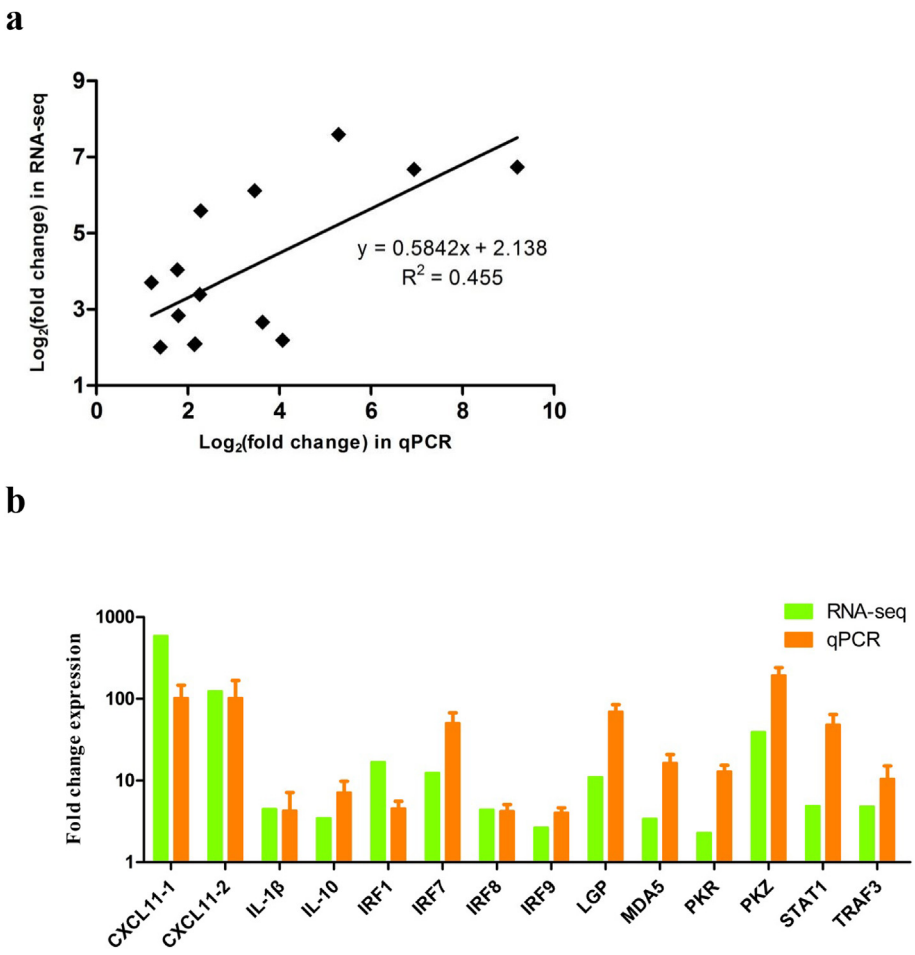

Fig. 7. Validation of RNA-seq data by qPCR. (a) Correlation of the expression levels of 14 IRDs acquired by RNA-seq and qPCR. (b) Comparison of the fold change expression of 14 selected DEGs as determined by RNA-seq and qPCR.

Meanwhile, IRF8 was potently induced at 4, 8, and 12 h, suggesting that IRF8 involves in the early phase of pIC-activated signaling cascades. Indeed, it has been reported that the transcript levels of IRF8 in turbot were also up-regulated with the pIC as a quicker inducer [57]. Furthermore, it has been demonstrated that pIC can induce three sequential waves of type I IFNs in mice, and the secondary late IFNs wave (IFN-α6T and-α6/8 after 6 h) is associated with the up-regulated of IRF8, while IRF7 is up-regulated in the late wave [58]. These evidences reveal that IRF8 may induce the early phase of the transcription of type I IFNs after pIC treatment. IRF9, a well-known IFN-stimulated gene factor 3 (ISGF3) in Jak-stat signaling pathway, was markedly up-regulated after pIC treatment at each time point in this study. Accumulating evidences highlight IRF9 implicates Jak-stat pathway by interacting with STAT molecules to induce ISGs in antiviral response [43,44]. Accordingly, we inferred that IRF9 is directly associated with the expression of ISGs to fight against persistent virus in *S. prenanti.*

In the present study, pIC treatment resulted in the up-regulation of the key components of MDA5-mediated signaling pathway such as MDA5, LGP2 and TRAF3. Previous studies had demonstrated that MDA5 directly binds the virus components (dsRNA) with the assist of LGP2, and triggers the downstream signaling molecule TRAF3, which leads to phosphorylation of IRF3/7, following inducing the production of type I IFNs [21]. Therefore, our results indicate the antiviral immune response of *S. prenanti* may be mediated by type I IFNs response, which is activated by MDA5-mediated signaling pathway. Remarkably, LGP2 exhibited a higher expression change than MDA5 and TRAF3, over 30-fold change at all examined time points, after pIC treatment. Despite lacking of CARDs domain and disabled in directly interacting with virus components [24], our qPCR data suggest that LGP2 may play a more important role in the initiative signaling transduction compare to MDA5. In addition, STAT1 was significantly up-regulated with time dependency, which involves in the Jak-stat signaling pathway to induce the ISGs containing Mx1, PKR and so on. Meanwhile, we also observed IRF9 was up-regulated in both of RNA-seq and qPCR results, while the transcript level of STAT2 was increased in RNA-seq data. Jak-stat pathway has been proved to be a crucial role in both innate and adaptive immunity [59]. And, STATs/IRF9 are known to mediate this signaling cascade by their dipolymer/tripolymer to regulate ISGs production [43,44,60]. Therefore, our results suggest that these effectors result in the up-regulated of ISGs (PKR and Mx1), but what complexes they formed and how to perform its function to mediate ISGs expression remains to be investigated in future study. In consistent with previous study, PKR and Mx1 were responsive to pIC stimulation in this study [39]. At the same time, PKZ exhibited a higher expression change, over 40-fold change at each time point, after pIC treatment. To our knowledge, PKZ, a homolog of PKR, performs the same function to shut down protein translation upon detection of viral dsRNA, although primary studies proved that it recognizes Z-DNA instead of dsRNA [61–63]. Therefore, like PKR, PKZ may also sever as a member of ISGs to inhibits virus replication.

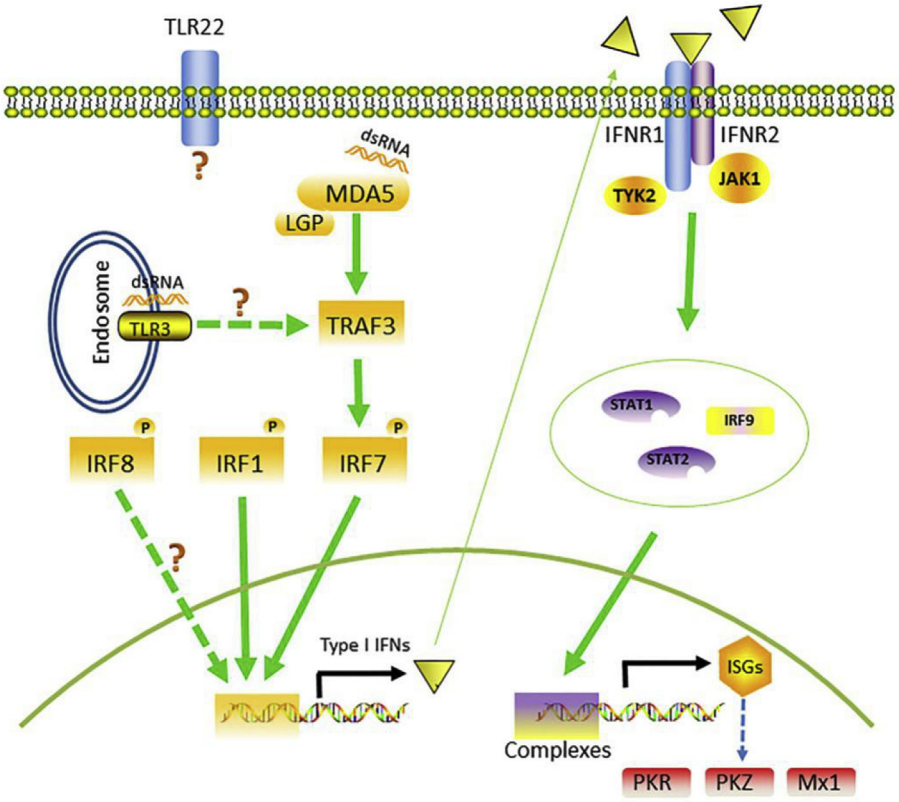

Fig. 8. The prediction of signaling pathways of the antiviral immune response in *Schizothorax prenanti*. The virus dsRNA is recognized by MDA5, which triggers the downstream signaling cascades, and finally induces ISGs to suppress virus replication in the cytoplasm. All the genes in map were up-regulated, except TLR22 and TLR3, according to RNA-seq and qPCR results. Moreover, whether TLR22, TLR3 and IRF8 are directly involved in these signaling transduction cascades remains to be investigated in future study, and marked by the dotted line and the question mark.

Moreover, IRF8 mRNA was significantly up-regulated after pIC treatment. It has been reported that pIC induced the up-regulation of IRF8 expression in both of teleost and mammals [54,57]. However, whether IRF8 directly involves in the signaling transduction of type I IFNs response is still unclear. TLR3, identified in the endosome of mammals and teleost, recognizes viral dsRNA intermediates and submits initiative signaling to downstream signaling cascades [64]. TLR22, a member of TLRs identified in aquatic animals, recognizes RNA duplex to induce type I IFNs response [65]. Surprisingly, our RNA-seq data showed that no significantly expression changes of TLR3 and TLR22 were detected after pIC treatment. Based on published research, TLR3 is exclusively expressed by dendritic cells (DC) [66], suggesting that TLR3 may recognize the viral dsRNA in the late phase but not at 12 h. As mentioned previously, the length of dsRNA affects TLR22-mediated antiviral signaling cascades, and the greatest length is about 1000bp [65]. Thus, this may be the reason why TLR22 was not activated by pIC treatment in *S. prenanti*, but the mechanism of *S. prenanti* TLR22 in antiviral response need be investigated in detail.

In summary, we identified DEGs in *S. prenanti* after pIC treatment. After RNA-seq data analysis and qPCR validation, we have observed that the antiviral immunity may be mediated by MDA- and Jak-mediated signaling pathways. Some well-known immune effectors such as IRF8 and IRF1 involve in aforesaid pathway, but whether they directly mediate the signaling transduction of aforesaid pathway remains to be investigated in future study. Remarkably, the expression of TLR3 and TLR22 was not influenced in our study, despite they are believed to be a promotor in antiviral immunity [64,65]. These questions may be dragged in future studies, which may clearly reveal the antiviral immunity of *S. prenanti*.

Acknowledgements

This work was supported in part by Two Sides Supporting Plan in Sichuan Agriculture University (00770103).

References

[1] X. Mu, J.W. Pridgeon, P.H. Klesius, Comparative transcriptional analysis reveals distinct expression patterns of channel catfish genes after the first infection and re-infection with Aeromonas hydrophila, Fish. Shellfish Immunol. 35 (2013) 1566–1576.
[2] Y. Geng, K.Y. Wang, X.L. Huang, D.F. Chen, C.W. Li, S.Y. Ren, et al., Streptococcus agalactiae, an emerging pathogen for cultured ya-fish, Schizothorax prenanti, in China, Transbound. Emerg. Dis. 59 (2012) 369–375.
[3] M.P. Polinski, J.C. Bradshaw, S.M. Inkpen, J. Richard, C. Fritsvold, T.T. Poppe, et al., De novo assembly of Sockeye salmon kidney transcriptomes reveal a limited early response to piscine reovirus with or without infectious hematopoietic necrosis virus superinfection, BMC Genomics 17 (2016) 848.
[4] M. Chen, H. Wang, Q. Yan, Q. Zheng, M. Yang, Z. Lv, et al., Effects of dietary oxidized konjac glucomannan sulfates (OKGMS) and acidolysis-oxidized konjac glucomannan (A-OKGM) on the immunity and expression of immune-related genes of Schizothorax prenanti, Fish. Shellfish Immunol. 56 (2016) 96–105.
[5] Q. Zheng, Y. Wu, H. Xu, H. Wang, H. Tang, X. Xia, et al., Immune responses to Aeromonas hydrophila infection in Schizothorax prenanti fed with oxidized konjac glucomannan and its acidolysis products, Fish. Shellfish Immunol. 49 (2016) 260–267.
[6] Q. Zheng, Y. Wu, H. Xu, Y. Yao, X. Xia, J. Feng, et al., The effects of dietary oxidized konjac glucomannan and its acidolysis products on the immune response, expression of immune related genes and disease resistance of Schizothorax prenanti, Fish. Shellfish Immunol. 45 (2015) 551–559.
[7] D. Yuan, T. Wang, C. Zhou, F. Lin, H. Chen, H. Wu, et al., Leptin and cholecystokinin in Schizothorax prenanti: molecular cloning, tissue expression, and

mRNA expression responses to periprandial changes and fasting, Gen. Comp. Endocrinol. 204 (2014) 13–24.
[8] J.D. Hansen, K.J. Vojtech, Ln Fau-Laing, K.J. Laing, Sensing disease and danger: a survey of vertebrate PRRs and their origins, Dev. Comp. Immunol. 35 (2011) 886–897.
[9] S. Jensen, A.R. Thomsen, Sensing of RNA viruses: a review of innate immune receptors involved in recognizing RNA virus invasion, J. Virol. 86 (2012) 2900–2910.
[10] E. Maverakis, K. Kim, M. Shimoda, M.E. Gershwin, F. Patel, R. Wilken, et al., Glycans in the immune system and the altered glycan theory of autoimmunity: a critical review, J. Autoimmun. 57 (2015) 1–13.
[11] T. Kawai, S. Akira, The roles of TLRs, RLRs and NLRs in pathogen recognition, Int. Immunol. 21 (2009) 317–337.
[12] A. Pichlmair, C. Reis e Sousa, Innate recognition of viruses, Immunity 27 (2007) 370–383.
[13] J. Zhang, X. Kong, C. Zhou, L. Li, G. Nie, X. Li, Toll-like receptor recognition of bacteria in fish: ligand specificity and signal pathways, Fish. Shellfish Immunol. 41 (2014) 380–388.
[14] K. Takeda, S. Akira, Toll-like receptors in innate immunity, Int. Immunol. 17 (2005) 1–14.
[15] S. Akira, Toll-like receptors and innate immunity, Adv. Immunol. 78 (2001) 1–56.
[16] B. Manavalan, S. Basith, S. Choi, Similar structures but different roles - an updated perspective on TLR structures, Front. Physiol. 2 (2011) 41.
[17] G.M. Barton, R. Medzhitov, Toll-like receptor signaling pathways, Science 300 (2003) 1524–1525.
[18] Y.B. Zhang, J.F. Gui, Molecular regulation of interferon antiviral response in fish, Dev. Comp. Immunol. 38 (2012) 193–202.
[19] A.M. Bruns, C.M. Horvath, Antiviral RNA recognition and assembly by RLR family innate immune sensors, Cytokine Growth Factor Rev. 25 (2014) 507–512.
[20] S. Reikine, J.B. Nguyen, Y. Modis, Pattern recognition and signaling mechanisms of RIG-I and MDA5, Front. Immunol. 5 (2014) 342.
[21] O. Takeuchi, S. Akira, MDA5/RIG-I and virus recognition, Curr. Opin. Immunol. 20 (2008) 17–22.
[22] H. Kato, O. Takeuchi, S. Sato, M. Yoneyama, M. Yamamoto, K. Matsui, et al., Differential roles of MDA5 and RIG-I helicases in the recognition of RNA viruses, Nature 441 (2006) 101–105.
[23] H. Kato, O. Takeuchi, E. Mikamo-Satoh, R. Hirai, T. Kawai, K. Matsushita, et al., Length-dependent recognition of double-stranded ribonucleic acids by retinoic acid-inducible gene-I and melanoma differentiation-associated gene 5, J. Exp. Med. 205 (2008) 1601–1610.
[24] M. Yoneyama, M. Kikuchi, K. Matsumoto, T. Imaizumi, M. Miyagishi, K. Taira, et al., Shared and unique functions of the DExD/H-box helicases RIG-I, MDA5, and LGP2 in antiviral innate immunity, J. Immunol. 175 (2005) 2851–2858.
[25] S. Deddouche, D. Goubau, J. Rehwinkel, P. Chakravarty, S. Begum, P.V. Maillard, et al., Identification of an LGP2-associated MDA5 agonist in picornavirus-infected cells, Elife 3 (2014) e01535.
[26] M. Chang, B. Collet, P. Nie, K. Lester, S. Campbell, C.J. Secombes, et al., Expression and functional characterization of the RIG-I-like receptors MDA5 and LGP2 in Rainbow trout (Oncorhynchus mykiss), J. Virol. 85 (2011) 8403–8412.
[27] K.R. Rodriguez, A.M. Bruns, C.M. Horvath, MDA5 and LGP2: accomplices and antagonists of antiviral signal transduction, J. Virol. 88 (2014) 8194–8200.
[28] B. Collet, C.J. Secombes, The rainbow trout (Oncorhynchus mykiss) Mx1 promoter. Structural and functional characterization, Eur. J. Biochem. 268 (2001) 1577–1584.
[29] J. D'Cunha, S. Ramanujam, R.J. Wagner, P.L. Witt, E. Knight Jr., E.C. Borden, In vitro and in vivo secretion of human ISG15, an IFN-induced immunomodulatory cytokine, J. Immunol. 157 (1996) 4100–4108.
[30] R. Zhu, Y.B. Zhang, Q.Y. Zhang, J.F. Gui, Functional domains and the antiviral effect of the double-stranded RNA-dependent protein kinase PKR from Paralichthys olivaceus, J. Virol. 82 (2008) 6889–6901.
[31] M.G. Grabherr, B.J. Haas, M. Yassour, J.Z. Levin, D.A. Thompson, I. Amit, et al., Trinity: reconstructing a full-length transcriptome without a genome from RNA-Seq data, Nat. Biotechnol. 29 (2013) 644–652.
[32] C. Camacho, G. Coulouris, V. Avagyan, N. Ma, J. Papadopoulos, K. Bealer, et al., BLAST+: architecture and applications, BMC Bioinforma. 10 (2009) 421.
[33] A. Conesa, S. Gotz, J.M. Garcia-Gomez, J. Terol, M. Talon, M. Robles, Blast2GO: a universal tool for annotation, visualization and analysis in functional genomics research, Bioinformatics 21 (2005) 3674–3676.
[34] B. Li, C.N. Dewey, RSEM: accurate transcript quantification from RNA-Seq data with or without a reference genome, BMC Bioinforma. 12 (2011) 93–99.
[35] C. Trapnell, B.A. Williams, G. Pertea, A. Mortazavi, G. Kwan, M.J. van Baren, et al., Transcript assembly and quantification by RNA-Seq reveals unannotated transcripts and isoform switching during cell differentiation, Nat. Biotechnol. 28 (2010) 511–515.
[36] W. Deng, Y. Wang, Z. Liu, H. Cheng, Y. Xue, HemI: a toolkit for illustrating heatmaps, PLoS One 9 (2014) e111988.
[37] K. Honda, A. Takaoka, T. Taniguchi, Type I interferon [corrected] gene induction by the interferon regulatory factor family of transcription factors, Immunity 25 (2006) 349–360.
[38] K. Honda, T. Taniguchi, IRFs: master regulators of signalling by Toll-like receptors and cytosolic pattern-recognition receptors, Nat. Rev. Immunol. 6 (2006) 644–658.
[39] Q. Chu, Y. Gao, G. Xu, C. Wu, T. Xu, Transcriptome comparative analysis revealed poly(I: C) activated RIG-I/MDA5-mediated signaling pathway in miiuy croaker, Fish. Shellfish Immunol. 47 (2015) 168–174.
[40] F. Sun, Y.B. Zhang, T.K. Liu, J. Shi, B. Wang, J.F. Gui, Fish MITA serves as a mediator for distinct fish IFN gene activation dependent on IRF3 or IRF7, J. Immunol. 187 (2011) 2531–2539.
[41] B. Huang, Z.T. Qi, Z. Xu, P. Nie, Global characterization of interferon regulatory factor (IRF) genes in vertebrates: glimpse of the diversification in evolution, BMC Immunol. 11 (2010) 22.
[42] K. Honda, H. Yanai, H. Negishi, M. Asagiri, M. Sato, T. Mizutani, et al., IRF-7 is the master regulator of type-I interferon-dependent immune responses, Nature 434 (2005) 772–777.
[43] K. Blaszczyk, H. Nowicka, K. Kostyrko, A. Antonczyk, J. Wesoly, H.A. Bluyssen, The unique role of STAT2 in constitutive and IFN-induced transcription and antiviral responses, Cytokine Growth Factor Rev. 29 (2016) 71–81.
[44] K. Fink, N. Grandvaux, STAT2 and IRF9: beyond ISGF3, JAKSTAT 2, 2013, p. e27521.
[45] B. Magnadottir, Innate immunity of fish (overview), Fish. Shellfish Immunol. 20 (2006) 137–151.
[46] Y. Rao, J. Su, Insights into the antiviral immunity against grass carp (Ctenopharyngodon idella) reovirus (GCRV) in grass carp, J. Immunol. Res. 2015 (2015).
[47] S. Chattopadhyay, G.C. Sen, dsRNA-activation of TLR3 and RLR signaling: gene induction-dependent and independent effects, J. Interferon Cytokine Res. 34 (2014) 427–436.
[48] L.F. Neville, G. Mathiak, O. Bagasra, The immunobiology of interferon-gamma inducible protein 10 kD (IP-10): a novel, pleiotropic member of the C-X-C chemokine superfamily, Cytokine Growth Factor Rev. 8 (1997) 207–219.
[49] O. Yoshie, T. Imai, H. Nomiyama, Chemokines in immunity, Adv. Immunol. 78 (2001) 57–110.
[50] M. Saraiva, A. O'Garra, The regulation of IL-10 production by immune cells, Nat. Rev. Immunol. 10 (2010) 170–181.
[51] K. Taga, H. Mostowski, G. Tosato, Human interleukin-10 can directly inhibit T-cell growth, Blood 81 (1993) 2964–2971.
[52] H. Groux, M. Bigler, J.E. de Vries, M.G. Roncarolo, Inhibitory and stimulatory effects of IL-10 on human CD8+ T cells, J. Immunol. 160 (1998) 3188–3193.
[53] L. Grayfer, J.W. Hodgkinson, S.J. Hitchen, M. Belosevic, Characterization and functional analysis of goldfish (Carassius auratus L.) interleukin-10, Mol. Immunol. 48 (2011) 563–571.
[54] K. Eslamloo, X. Xue, M. Booman, N.C. Smith, M.L. Rise, Transcriptome profiling of the antiviral immune response in Atlantic cod macrophages, Dev. Comp. Immunol. 63 (2016) 187–205.
[55] M. Miyamoto, T. Fujita, Y. Kimura, M. Maruyama, H. Harada, Y. Sudo, et al., Regulated expression of a gene encoding a nuclear factor, IRF-1, that specifically binds to IFN-beta gene regulatory elements, Cell 54 (1988) 903–913.
[56] S. Ning, J.S. Pagano, G.N. Barber, IRF7: activation, regulation, modification and function, Genes Immun. 12 (2011) 399–414.
[57] X. Chen, G. Hu, X. Dong, Q. Liu, S. Zhang, Molecular cloning and expression analysis of interferon regulatory factor 8 (IRF8) in turbot, Scophthalmus maximus, Vet. Immunol. Immunopathol. 149 (2012) 143–150.
[58] T. Demoulins, M.L. Baron, N. Kettaf, A. Abdallah, E. Sharif-Askari, R.P. Sekaly, Poly (I: C) induced immune response in lymphoid tissues involves three sequential waves of type I IFN expression, Virology 386 (2009) 225–236.
[59] K. Ghoreschi, A. Laurence, J.J. O'Shea, Janus kinases in immune cell signaling, Immunol. Rev. 228 (2009) 273–287.
[60] D.E. Levy, D.S. Kessler, R. Pine, J.E. Darnell Jr., Cytoplasmic activation of ISGF3, the positive regulator of interferon-alpha-stimulated transcription, reconstituted in vitro, Genes Dev. 3 (1989) 1362–1371.
[61] S. Rothenburg, N. Deigendesch, K. Dittmar, F. Koch-Nolte, F. Haag, K. Lowenhaupt, et al., A PKR-like eukaryotic initiation factor 2alpha kinase from zebrafish contains Z-DNA binding domains instead of dsRNA binding domains, Proc. Natl. Acad. Sci. U. S. A. 102 (2005) 1602–1607.
[62] D. Kim, J. Hur, K. Park, S. Bae, D. Shin, S.C. Ha, et al., Distinct Z-DNA binding mode of a PKR-like protein kinase containing a Z-DNA binding domain (PKZ), Nucleic Acids Res. 42 (2014) 5937–5948.
[63] V. Bergan, R. Jagus, S. Lauksund, O. Kileng, B. Robertsen, The Atlantic salmon Z-DNA binding protein kinase phosphorylates translation initiation factor 2 alpha and constitutes a unique orthologue to the mammalian dsRNA-activated protein kinase R, FEBS J. 275 (2008) 184–197.
[64] S. Poynter, G. Lisser, A. Monjo, S. DeWitte-Orr, Sensors of infection: viral nucleic acid PRRs in fish, Biol. (Basel) 4 (2015) 460–493.
[65] A. Matsuo, H. Oshiumi, T. Tsujita, H. Mitani, H. Kasai, M. Yoshimizu, et al., Teleost TLR22 recognizes RNA duplex to induce IFN and protect cells from birnaviruses, J. Immunol. 181 (2008) 3474–3485.
[66] M. Muzio, D. Bosisio, N. Polentarutti, G. D'Amico, A. Stoppacciaro, R. Mancinelli, et al., Differential expression and regulation of toll-like receptors (TLR) in human leukocytes: selective expression of TLR3 in dendritic cells, J. Immunol. 164 (2000) 5998–6004.